Available online at www.sciencedirect.com
SCIENCE DIRECT®
Comput. Methods Appl. Mech. Engrg. 193 (2004) 4207–4222
Computer methods in applied mechanics and engineering
www.elsevier.com/locate/cma

An ALE formulation based on spatial and material settings of continuum mechanics. Part 1: Generic hyperelastic formulation

Ellen Kuhl [a], Harm Askes [b], Paul Steinmann [a,*]

[a] *Department of Mechanical Engineering, Faculty of Mechanical Engineering, Chair of Applied Mechanics, University of Kaiserslautern, P.O. Box 3049, D-67653 Kaiserslautern, Germany*

[b] *Faculty of Civil Engineering and Geosciences, Delft University of Technology, P.O. Box 5048, NL-2600 Delft, The Netherlands*

Received 16 May 2003; received in revised form 23 August 2003; accepted 4 September 2003

Abstract

The present contribution deals with the derivation of a generic hyperelastic Arbitrary Lagrangian–Eulerian formulation on the basis of a consistent variational framework. The governing equations follow straightforwardly from the Dirichlet principle for conservative mechanical systems. Thereby, the key idea is the reformulation of the total variation of the potential energy at fixed referential coordinates in terms of its variation at fixed material and at fixed spatial coordinates. The corresponding Euler–Lagrange equations define the spatial and the material motion version of the balance of linear momentum, i.e. the balance of spatial and material forces, in a consistent dual format. In the discretised setting, the governing equations are solved simultaneously rendering the spatial and the material configuration which minimise the overall potential energy of the system. The remeshing strategy of the ALE formulation is thus no longer user-defined but objective in the sense of energy minimisation. If the governing equations are derived from a potential, i.e. either from an incremental potential or from a total potential as in the present case, they are inherently symmetric, both in the continuous case and in the discrete case. This symmetry property is particularly appealing since it ensures symmetric system matrices upon discretisation.

Keywords: Arbitrary Lagrangian–Eulerian formulation; Spatial and material settings; Variational principle; Spatial and material forces; Finite element method

1. Introduction

Historically, two fundamental frameworks to describe the relevant kinematics have dominated continuum mechanics research and applications. Firstly, one can follow the material in time and describe motion

* Corresponding author. Tel.: +49-631-205-2419; fax: +49-631-205-2128.
E-mail addresses: ekuhl@rhrk.uni-kl.de (E. Kuhl), h.askes@citg.tudelft.nl (H. Askes), ps@rhrk.uni-kl.de (P. Steinmann).
URL: http://mechanik.mv.uni-kl.de.

0045-7825/$ - see front matter
doi:10.1016/j.cma.2003.09.030

and deformation by registration of the successive spatial positions that each physical 'particle' occupies. This approach is commonly known as the *Lagrangian description*, and it is primarily used by the solid mechanics community. Secondly, one can attain a fixed position in space and record the flow of physical 'particles' along this point in order to describe motion and deformation of matter. The latter approach is normally termed the *Eulerian description*, and it is mainly used in fluid mechanics.

This separation in approaches for solid mechanics and fluid mechanics has been carried over to the numerical applications that have emerged in more recent years. However, it has long been recognised that Lagrangian and Eulerian descriptions of continuum behaviour have their limitations in case numerical solution strategies are taken. For instance, in Lagrangian finite element meshes the nodes are attached one-to-one to the material particles. Therefore, excessive deformation of the material invariably leads to excessive deformation of the mesh, which may result in element entanglement and singularities in the isoparametric mapping of the elements. On the other hand, Eulerian grids are attached one-to-one to space, so that large boundary motion of the material cannot be accounted for accurately. Furthermore, a difficulty arises when fluid–structure interaction is considered: when the fluid is described by a Eulerian method and the structure by a Lagrangian method, an ambiguity pertains for the interface zone.

To combine the advantages and to avoid the limitations of either approach, *Arbitrary Lagrangian–Eulerian* (ALE) approaches have been proposed in the literature, see e.g. the early approaches by Donéa et al. [1], Belytschko and Kennedy [2], Donéa [3,4], Hughes et al. [5] or Liu [6] or the more recent work of Huerta and Casadei [7], Belytschko et al. [8], Wall [9], Braess and Wriggers [10], Rodríguez-Ferran et al. [11], Donéa and Huerta [12] and Kuhl et al. [13]. For more sophisticated applications in the context of mesh adaptivity, we refer to Pijaudier-Cabot et al. [14], the recent works of Askes et al. [15–19], Yamada and Kikuchi [20] and Armero and Love [21]. As is implied by this denotation, an ALE approach is neither purely Lagrangian (i.e. nodes of a grid are not attached to the material) nor is it purely Eulerian (i.e. nodes of a grid are not fixed in space). In contrast, nodes are free to move in space *independently of the material*. Whereas the motion of the material is set by the applicable equations of mechanics, the motion of the nodes has to be prescribed by the user. As such, the motion of the nodes has become an additional unknown.

It is instructive to notice that in most solid mechanics ALE applications, a so-called uncoupled or *staggered* solution scheme is chosen. Then, within a time step two substeps are taken: firstly, mesh motion is neglected and the equations of mechanics are solved by a purely Lagrangian substep; secondly, the mesh motion is determined and the state variables are transferred from the old mesh positions to the new mesh positions via a purely Eulerian (convective) substep. In other words, firstly the motion of material particles in space is followed, and secondly the convection of material along fixed points in space is tracked.

The issue of the Lagrangian and Eulerian viewpoint is strongly related to the *spatial* and *material* setting of continuum mechanics as illustrated e.g in the recent textbooks by Maugin [22], Gurtin [23] and Kienzler and Herrmann [24] and Silhavý [25] or in the excellent monographs by Maugin [26] and Gurtin [27]. Within the former approach, spatial placements of physical particles are followed through the surrounding space at fixed material position while the latter approach is based on the analysis of changes in the material placement of particles relative to the ambient material at fixed spatial position. In this context, two completely dual formulations can be derived whereby the former, the mechanics on the spatial manifold, is typically referred to as Newtonian mechanics whereas the latter format is often referred to as mechanics on the material manifold or Eshelbian mechanics. This aspect of duality has been highlighted first by Shield [28] and was elaborated further recently in our own group, see Steinmann [29–32] and Kuhl et al. [33].

While the spatial motion problem typically deals with spatial or Newtonian forces which are essentially conjugate to spatial variations at fixed material positions, material or Eshelbian forces are generated by material variations at fixed positions in the spatial configuration. Classically, material forces were introduced in the context of material inhomogeneities, e.g. cracks or dislocations. The original work of Eshelby [34,35] thus deals with the forces acting on *continuum* defects or singularities. The first discussion on *discrete* material forces introduced by the finite element discretisation dates back to Braun [36]. In this context,

finite element nodes can be interpreted as discrete defects inducing discrete material forces. Meshing can thus be improved by moving the nodes in the direction opposite the corresponding material forces and thus further lowering the overall energy, see Mueller and Maugin [37], Askes et al. [19], Thoutireddy and Ortiz [38] and Thoutireddy [39]. Vanishing material node point forces thus correspond to optimal meshes, i.e. meshes which render a minimum in potential energy. In contrast to heuristically formulated ALE-based remeshing strategies, the approach suggested herein is strictly embedded in a variational framework and thus renders symmetric system matrices upon discretisation. Moreover, the remeshing strategy follows straightforwardly from the evaluation of the variational principle, such that no additional user-defined remeshing parameters need to be introduced.

The present contribution is organised as follows. After reviewing the relevant ALE kinematics in Section 2, we will illustrate the variational framework of our ALE formulation based on the ALE Dirichlet principle in Section 3. The variations of the total potential energy with respect to the spatial coordinates at fixed material position and with respect to the material coordinates at fixed spatial position render the corresponding spatial and material version of the Euler–Lagrange equations, a non-linear set of equations which will be linearised in Section 4. Section 5 finally treats its spatial discretisation in terms of the material and the spatial reference mapping. A first discussion of this generic formulation will be given in Section 6, whereas a specification to a classical compressible Neo–Hooke material model and related computational issues are treated in Part 2 of this contribution by Askes et al. [40].

2. ALE kinematics

Let us briefly summarise the fundamental kinematic relations of the present ALE formulation which is basically characterised through the introduction of an independent fixed reference domain $\mathscr{B}_\square$ next to the classical material and spatial domain $\mathscr{B}_0$ and $\mathscr{B}_t$. Thereby, any scalar- or tensor-valued quantity per unit volume in either $\mathscr{B}_\square$, $\mathscr{B}_0$ or $\mathscr{B}_t$ will be denoted as $\{\bullet\}_\square$, $\{\bullet\}_0$ or $\{\bullet\}_t$, respectively. The following considerations are essentially based on two independent mappings, i.e. the referential maps from the fixed referential configuration $\mathscr{B}_\square$ to the material configuration $\mathscr{B}_0$ and from the referential configuration $\mathscr{B}_\square$ to the spatial configuration $\mathscr{B}_t$ as illustrated in Fig. 1. Let $\tilde{\boldsymbol{\Phi}}$ with

$$\boldsymbol{X} = \tilde{\boldsymbol{\Phi}}(\boldsymbol{\xi}, t) : \mathscr{B}_\square \to \mathscr{B}_0 \tag{1}$$

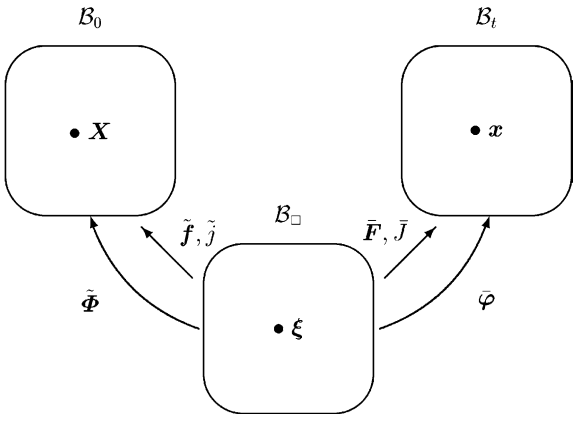

Fig. 1. Referential maps and referential tangent maps.

denote the mapping of physical particles from a fixed position $\boldsymbol{\xi}$ in the referential domain $\mathscr{B}_\square$ to their material position $\boldsymbol{X}$ in the material domain $\mathscr{B}_0$. Its referential gradient $\tilde{\boldsymbol{f}}$

$$\tilde{\boldsymbol{f}} = \nabla_{\boldsymbol{\xi}} \tilde{\boldsymbol{\Phi}}(\boldsymbol{\xi}, t) : T\mathscr{B}_\square \rightarrow T\mathscr{B}_0 \quad \tilde{j} = \det \tilde{\boldsymbol{f}} > 0 \tag{2}$$

defines the related tangent map from the referential tangent space $T\mathscr{B}_\square$ to the material tangent space $T\mathscr{B}_0$ with the related Jacobian $\tilde{j}$. With $\tilde{j} > 0$, we assure the existence of the inverse map $\tilde{\boldsymbol{\varphi}}$ with $\boldsymbol{\xi} = \tilde{\boldsymbol{\varphi}}(\boldsymbol{X}, t) : \mathscr{B}_0 \rightarrow \mathscr{B}_\square$ whereby $\tilde{\boldsymbol{F}} = \nabla_{\boldsymbol{X}} \tilde{\boldsymbol{\varphi}}(\boldsymbol{X}, t) = \tilde{\boldsymbol{f}}^{-1} : T\mathscr{B}_0 \rightarrow T\mathscr{B}_\square$ with $\tilde{J} = \det \tilde{\boldsymbol{F}} = 1/\tilde{j} > 0$. Moreover, we introduce the second independent mapping $\bar{\boldsymbol{\varphi}}$ from the referential domain $\mathscr{B}_\square$ to the spatial domain $\mathscr{B}_0$.

$$\boldsymbol{x} = \bar{\boldsymbol{\varphi}}(\boldsymbol{\xi}, t) : \mathscr{B}_\square \rightarrow \mathscr{B}_t. \tag{3}$$

The related referential gradient $\bar{\boldsymbol{F}}$ and its Jacobian $\bar{J}$

$$\bar{\boldsymbol{F}} = \nabla_{\boldsymbol{\xi}} \bar{\boldsymbol{\varphi}}(\boldsymbol{\xi}, t) : T\mathscr{B}_\square \rightarrow T\mathscr{B}_t \quad \bar{J} = \det \bar{\boldsymbol{F}} > 0 \tag{4}$$

characterise the corresponding tangent map from the referential tangent space $T\mathscr{B}_\square$ to the spatial tangent space $T\mathscr{B}_t$. The related inverse map $\bar{\boldsymbol{\Phi}}$ can be expressed as $\boldsymbol{\xi} = \bar{\boldsymbol{\Phi}}(\boldsymbol{x}, t) : \mathscr{B}_t \rightarrow \mathscr{B}_\square$ with $\bar{\boldsymbol{f}} = \nabla_{\boldsymbol{x}} \bar{\boldsymbol{\Phi}}(\boldsymbol{x}, t) = \bar{\boldsymbol{F}}^{-1} : T\mathscr{B}_t \rightarrow T\mathscr{B}_\square$ and $\bar{j} = \det \bar{\boldsymbol{f}} = 1/\bar{J} > 0$. The variation and the linearisation at fixed referential coordinate $\boldsymbol{\xi}$ denoted as $\delta\{\bullet\} = \delta\{\bullet\}|_{\boldsymbol{\xi}\text{fixed}}$ and $\Delta\{\bullet\} = \Delta\{\bullet\}|_{\boldsymbol{\xi}\text{fixed}}$ will be referred to as total variation and total linearisation in the sequel. They can be expressed as the variation or linearisation with respect to the spatial coordinates $\boldsymbol{x}$ at fixed material coordinates $\boldsymbol{X}$ denoted as $\delta_{\boldsymbol{x}}\{\bullet\}$ or $\Delta_{\boldsymbol{x}}\{\bullet\}$, respectively, plus a contribution with respect to the material coordinates $\boldsymbol{X}$ at fixed spatial coordinates $\boldsymbol{x}$ denoted as $\delta_{\boldsymbol{X}}\{\bullet\}$ or $\Delta_{\boldsymbol{X}}\{\bullet\}$.

$$\delta\{\bullet\} = \delta_{\boldsymbol{x}}\{\bullet\} + \delta_{\boldsymbol{X}}\{\bullet\} \quad \Delta\{\bullet\} = \Delta_{\boldsymbol{x}}\{\bullet\} + \Delta_{\boldsymbol{X}}\{\bullet\}. \tag{5}$$

The individual contributions $\delta_{\boldsymbol{x}}\{\bullet\}$, $\delta_{\boldsymbol{X}}\{\bullet\}$, $\Delta_{\boldsymbol{x}}\{\bullet\}$ and $\Delta_{\boldsymbol{X}}\{\bullet\}$ will be defined in the following subsections. With these definitions at hand, we can now formulate the kinematics of the spatial and the material motion problem. For the former we typically follow spatial placements $\boldsymbol{x}$ of physical particles through the ambient space at fixed material position $\boldsymbol{X}$ corresponding to a Lagrangian viewpoint. For the latter, material placements $\boldsymbol{X}$ of physical particles are followed through the ambient material at fixed spatial position $\boldsymbol{x}$, the observer thus takes the Eulerian viewpoint. Recall, however, that neither the spatial nor the material deformation map represent an independent mapping in the present context since both can be reformulated in terms of the referential mappings defined above.

2.1. Spatial motion problem

In the spatial motion problem, the placement $\boldsymbol{x}$ of a physical particle in the spatial configuration $\mathscr{B}_t$ is described by the non-linear spatial deformation map $\boldsymbol{\varphi}$

$$\boldsymbol{x} = \boldsymbol{\varphi}(\boldsymbol{X}, t) = \bar{\boldsymbol{\varphi}}(\boldsymbol{\xi}, t) \circ \tilde{\boldsymbol{\varphi}}(\boldsymbol{X}, t) : \mathscr{B}_0 \rightarrow \mathscr{B}_t \tag{6}$$

in terms of the placement $\boldsymbol{X}$ in the material configuration $\mathscr{B}_0$, see Fig. 2.

It can thus be understood as a composition of the referential maps $\bar{\boldsymbol{\varphi}}$ and $\tilde{\boldsymbol{\varphi}}$. The related spatial motion deformation gradient $\boldsymbol{F}$, i.e. the linear tangent map associated with the spatial motion deformation map, is given as

$$\boldsymbol{F} = \nabla_{\boldsymbol{X}} \boldsymbol{\varphi}(\boldsymbol{X}, t) = \bar{\boldsymbol{F}} \cdot \tilde{\boldsymbol{F}} : T\mathscr{B}_0 \rightarrow T\mathscr{B}_t \quad J = \det \boldsymbol{F} = \bar{J}\tilde{J} > 0 \tag{7}$$

with J denoting the related Jacobian. Note that the spatial motion deformation gradient is essentially characterised through the multiplicative decomposition in terms of the referential gradients $\bar{\boldsymbol{F}}$ and $\tilde{\boldsymbol{F}}$. As typical strain measures of the spatial motion problem, we introduce the right and left spatial motion Cauchy–Green strain tensors $\boldsymbol{C} = \boldsymbol{F}^t \cdot \boldsymbol{F}$ and $\boldsymbol{b} = \boldsymbol{F} \cdot \boldsymbol{F}^t$, respectively. In what follows, the variation and

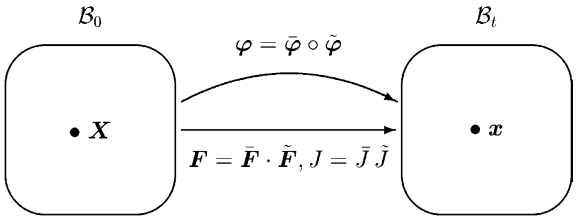

Fig. 2. Spatial deformation map and spatial tangent map.

linearisation of a function $\{\bullet\}$ with respect to the spatial coordinates $\vec{x}$ at fixed material coordinates $\boldsymbol{X}$ will be denoted as $\delta_x\{\bullet\} = \delta\{\bullet\}|_{\boldsymbol{X}\text{fixed}}$ and $\Delta_x\{\bullet\} = \Delta\{\bullet\}|_{\boldsymbol{X}\text{fixed}}$. Consequently, the variation and linearisation of the spatial motion deformation map and its gradient can be expressed in the following form.

$$\begin{aligned} &\delta_x\boldsymbol{\varphi} = \delta\bar{\boldsymbol{\varphi}} \quad \delta_x\boldsymbol{F} = \nabla_{\boldsymbol{X}}\delta\bar{\boldsymbol{\varphi}}, \\ &\Delta_x\boldsymbol{\varphi} = \Delta\bar{\boldsymbol{\varphi}} \quad \Delta_x\boldsymbol{F} = \nabla_{\boldsymbol{X}}\Delta\bar{\boldsymbol{\varphi}}. \end{aligned} \tag{8}$$

In the sequel, we will particularly make use of the following expressions,

$$\begin{aligned} &\delta_x\{\bullet\}_0(\boldsymbol{F},\boldsymbol{\varphi};\boldsymbol{X}) = \mathrm{D}_{\boldsymbol{F}}\{\bullet\}_0 : \nabla_{\boldsymbol{X}}\delta\bar{\boldsymbol{\varphi}} + \partial_x\{\bullet\}_0 \cdot \delta\bar{\boldsymbol{\varphi}}, \\ &\Delta_x\{\bullet\}_0(\boldsymbol{F},\boldsymbol{\varphi};\boldsymbol{X}) = \mathrm{D}_{\boldsymbol{F}}\{\bullet\}_0 : \nabla_{\boldsymbol{X}}\Delta\bar{\boldsymbol{\varphi}} + \partial_x\{\bullet\}_0 \cdot \Delta\bar{\boldsymbol{\varphi}} \end{aligned} \tag{9}$$

which relate the linearisation and variation of a scalar-valued function $\{\bullet\}_0$ with a possible dependence on the deformation gradient $\boldsymbol{F}$, the deformation map $\boldsymbol{\varphi}$ and the material position $\boldsymbol{X}$ to its derivative with respect to the deformation gradient $\mathrm{D}_{\boldsymbol{F}}\{\bullet\}_0$ and its explicit derivative with respect to the spatial coordinate $\partial_x\{\bullet\}_0$.

2.2. Material motion problem

In complete analogy to the spatial motion problem, we can introduce a material motion map $\boldsymbol{\Phi}$ defining the mapping of the placement $\boldsymbol{X}$ of physical particles in the material configuration $\mathscr{B}_0$

$$\boldsymbol{X} = \boldsymbol{\Phi}(\boldsymbol{x},t) = \tilde{\boldsymbol{\Phi}}(\boldsymbol{\xi},t) \circ \bar{\boldsymbol{\Phi}}(\boldsymbol{x},t) : \mathscr{B}_t \to \mathscr{B}_0 \tag{10}$$

in terms of the related placement $\boldsymbol{x}$ in the spatial configuration $\mathscr{B}_t$. As illustrated in Fig. 3, the material deformation map can thus be interpreted as a composition of the referential mappings $\tilde{\boldsymbol{\Phi}}$ and $\bar{\boldsymbol{\Phi}}$. The related linear tangent map from the spatial tangent space $T\mathscr{B}_t$ to the material tangent space $T\mathscr{B}_0$ is defined through the material motion deformation gradient $\boldsymbol{f}$ and its Jacobian j,

$$\boldsymbol{f} = \nabla_{\boldsymbol{x}}\boldsymbol{\Phi}(\boldsymbol{x},t) = \tilde{\boldsymbol{f}} \cdot \bar{\boldsymbol{f}} : T\mathscr{B}_t \to T\mathscr{B}_0 \quad j = \det\boldsymbol{f} = \tilde{j}\bar{j} > 0, \tag{11}$$

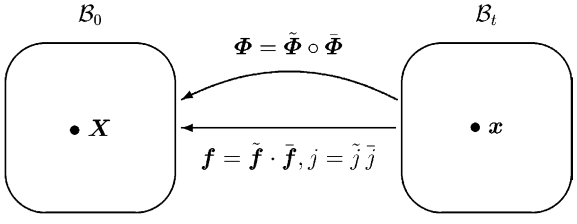

Fig. 3. Material deformation map and material tangent map.

whereby $\boldsymbol{f}$ can be decomposed multiplicatively in the referential gradients $\tilde{\boldsymbol{f}}$ and $\bar{\boldsymbol{f}}$. The right and left material motion Cauchy–Green strain tensors $\boldsymbol{c} = \boldsymbol{f}^t \cdot \boldsymbol{f}$ and $\boldsymbol{B} = \boldsymbol{f} \cdot \boldsymbol{f}^t$ represent characteristic strain measures of the material motion problem. The variation and the linearisation of any function $\{\bullet\}$ with respect to the material coordinates $\boldsymbol{X}$ at fixed spatial coordinates $\boldsymbol{x}$ denoted as $\delta_{\boldsymbol{X}}\{\bullet\} = \delta\{\bullet\}|_{\boldsymbol{x}\text{fixed}}$ and $\Delta_{\boldsymbol{X}}\{\bullet\} = \Delta\{\bullet\}|_{\boldsymbol{x}\text{fixed}}$ define the variation and linearisation of the material motion deformation map and its gradient in the following form.

$$\begin{aligned} &\delta_{\boldsymbol{X}}\boldsymbol{\Phi} = \delta\tilde{\boldsymbol{\Phi}} \quad \delta_{\boldsymbol{X}}\boldsymbol{f} = \nabla_{\boldsymbol{x}}\delta\tilde{\boldsymbol{\Phi}}, \\ &\Delta_{\boldsymbol{X}}\boldsymbol{\Phi} = \Delta\tilde{\boldsymbol{\Phi}} \quad \Delta_{\boldsymbol{X}}\boldsymbol{f} = \nabla_{\boldsymbol{x}}\Delta\tilde{\boldsymbol{\Phi}}. \end{aligned} \tag{12}$$

Moreover, we obtain the following relation

$$\begin{aligned} &\delta_{\boldsymbol{X}}\{\bullet\}_t(\boldsymbol{f}, \boldsymbol{\Phi}; \boldsymbol{x}) = \mathrm{d}_f\{\bullet\}_t : \nabla_{\boldsymbol{x}}\delta\tilde{\boldsymbol{\Phi}} + \partial_{\boldsymbol{X}}\{\bullet\}_t \cdot \delta\tilde{\boldsymbol{\Phi}}, \\ &\Delta_{\boldsymbol{X}}\{\bullet\}_t(\boldsymbol{f}, \boldsymbol{\Phi}; \boldsymbol{x}) = \mathrm{d}_f\{\bullet\}_t : \nabla_{\boldsymbol{x}}\Delta\tilde{\boldsymbol{\Phi}} + \partial_{\boldsymbol{X}}\{\bullet\}_t \cdot \Delta\tilde{\boldsymbol{\Phi}} \end{aligned} \tag{13}$$

between the variation and the linearisation of a scalar-valued function $\{\bullet\}_t$ as a function of $\boldsymbol{f}$, $\boldsymbol{\Phi}$ and $\boldsymbol{x}$, the related derivative with respect to the material motion deformation gradient $\mathrm{d}_f\{\bullet\}_t$ and the explicit derivative with respect to the material coordinate $\partial_{\boldsymbol{X}}\{\bullet\}_t$.

Remark 1 (*Spatial vs. material quantities*). In the continuous case, the spatial and the material motion problem are related through the identity maps in $\mathscr{B}_0$ and $\mathscr{B}_t$,

$$\boldsymbol{id}_{\mathscr{B}_0} = \boldsymbol{\Phi}(\boldsymbol{\varphi}(\boldsymbol{X}, t), t) \quad \boldsymbol{id}_{\mathscr{B}_t} = \boldsymbol{\varphi}(\boldsymbol{\Phi}(\boldsymbol{x}, t), t) \tag{14}$$

while the spatial and the material deformation gradient are simply related by their inverses.

$$\boldsymbol{f} = \boldsymbol{F}^{-1} = \tilde{\boldsymbol{f}} \cdot \bar{\boldsymbol{f}} \quad \boldsymbol{F} = \boldsymbol{f}^{-1} = \bar{\boldsymbol{F}} \cdot \tilde{\boldsymbol{F}}. \tag{15}$$

Scalar-valued or tensorial quantities with material reference $\{\bullet\}_0$ and spatial reference $\{\bullet\}_t$ are related through the well-known transformation formulae.

$$\{\bullet\}_t = j\{\bullet\}_0 = \tilde{j}\bar{j}\{\bullet\}_0 \quad \{\bullet\}_0 = J\{\bullet\}_t = \bar{J}\tilde{J}\{\bullet\}_t. \tag{16}$$

Moreover, the equivalences of vector- or tensor-valued material surface fluxes $\{\square\}$ through the boundary of the material domain $\partial\mathscr{B}_0$ and the corresponding spatial surface fluxes $\{\diamondsuit\}$ through the spatial boundary $\partial\mathscr{B}_t$ render the well-known Nanson's formulae.

$$\{\diamondsuit\} = j\{\square\} \cdot \boldsymbol{F}^t = \tilde{j}\bar{j}\{\square\} \cdot \tilde{\boldsymbol{F}}^t \cdot \bar{\boldsymbol{F}}^t \quad \{\square\} = J\{\diamondsuit\} \cdot \boldsymbol{f}^t = \bar{J}\tilde{J}\{\diamondsuit\} \cdot \bar{\boldsymbol{f}}^t \cdot \tilde{\boldsymbol{f}}^t. \tag{17}$$

Later on, we will further invoke the following relations between the derivative of a scalar-valued function $\{\bullet\}_0$ or $\{\bullet\}_t$ with respect to the spatial and material motion deformation gradient

$$\mathrm{D}_{\boldsymbol{F}}\{\bullet\}_0 = \{\bullet\}_0\boldsymbol{f}^t - J\boldsymbol{f}^t \cdot \mathrm{d}_f\{\bullet\}_t \cdot \boldsymbol{f}^t \quad \mathrm{d}_f\{\bullet\}_t = \{\bullet\}_t\boldsymbol{F}^t - j\boldsymbol{F}^t \cdot \mathrm{D}_{\boldsymbol{F}}\{\bullet\}_0 \cdot \boldsymbol{F}^t \tag{18}$$

which has been given earlier by Steinmann [30].

Remark 2 (*Lagragian vs. Eulerian viewpoint*). The classical Lagrangian and Eulerian viewpoint can be derived as special cases of the above formulation with keeping either $\tilde{\boldsymbol{\Phi}}$ or $\bar{\boldsymbol{\varphi}}$ fixed such that either $\boldsymbol{\varphi} = \bar{\boldsymbol{\varphi}}$ or $\boldsymbol{\Phi} = \tilde{\boldsymbol{\Phi}}$. In the first case corresponding the Lagrangian viewpoint, the referential configuration $\mathscr{B}_\square$ coincides with the material configuration $\mathscr{B}_0$ while in the second case, corresponding to the Eulerian viewpoint, the referential configuration $\mathscr{B}_\square$ coincides with the spatial configuration $\mathscr{B}_t$.

Remark 3 (*Rates of kinematic quantities*). The issue of rates of kinematic quantities which is closely related to the formulation of appropriate ALE transport theorems is beyond the scope of the present study. It becomes relevant in particular for transient problems which will are part of current research and will therefore be treated in a separate contribution.

3. ALE Dirichlet principle

In what follows, we shall restrict ourselves to the hyperelastostatic case for conservative systems for which the Dirichlet principle defines the appropriate variational setting. In this context, we introduce the internal potential energy density $W_\square$ per unit volume in $\mathscr{B}_\square$, which is typically referred to as strain energy density. Conservative loading is characterised through the external potential energy density for conservative systems $V_\square$ per unit volume in $\mathscr{B}_\square$.

$$\begin{aligned} W_\square(\bar{\boldsymbol{F}},\tilde{\boldsymbol{f}};\boldsymbol{\xi}) &= \tilde{j}W_0(\boldsymbol{F};\boldsymbol{X}) = \bar{J}W_t(\boldsymbol{f},\boldsymbol{\Phi}), \\ V_\square(\bar{\boldsymbol{\varphi}},\tilde{\boldsymbol{\Phi}};\boldsymbol{\xi}) &= \tilde{j}V_0(\boldsymbol{\varphi};\boldsymbol{X}) = \bar{J}V_t(\boldsymbol{\Phi};\boldsymbol{x}). \end{aligned} \tag{19}$$

The total potential energy density $U_\square$ per unit volume in $\mathscr{B}_\square$ can thus be expressed as the sum of the corresponding internal and external contribution $W_\square$ and $V_\square$ as $U_\square = W_\square + V_\square$.

$$U_\square(\bar{\boldsymbol{F}},\tilde{\boldsymbol{f}},\bar{\boldsymbol{\varphi}},\tilde{\boldsymbol{\Phi}};\boldsymbol{\xi}) = \tilde{j}U_0(\boldsymbol{F},\boldsymbol{\varphi};\boldsymbol{X}) = \bar{J}U_t(\boldsymbol{f},\boldsymbol{\Phi};\boldsymbol{x}). \tag{20}$$

Then, the conservative mechanical system is essentially characterised through the total energy $\mathscr{I}$ defined through the integration of $U_\square$ over the reference domain $\mathscr{B}_\square$,

$$\mathscr{I}(\bar{\boldsymbol{\varphi}},\tilde{\boldsymbol{\Phi}}) = \int_{\mathscr{B}_\square} U_\square \,\mathrm{d}V_\square \rightarrow \inf, \tag{21}$$

whereby, in this context, $\mathrm{d}V_\square$ denotes the volume differential element. The infimum of the total potential energy $\mathscr{I}$ corresponds to a vanishing total variation, i.e. the variation at fixed referential coordinates $\boldsymbol{\xi}$.

$$\delta\mathscr{I} = \delta_{\boldsymbol{x}}\mathscr{I} + \delta_{\boldsymbol{X}}\mathscr{I} = 0. \tag{22}$$

According to Eq. (5), this total variation consists of a variation with respect to the spatial coordinates $\boldsymbol{x}$ at fixed material coordinates $\boldsymbol{X}$ plus variation with respect to the material coordinates $\boldsymbol{X}$ at fixed spatial coordinates $\boldsymbol{x}$. These variations will be elaborated in detail in the sequel. Thereby, we will particularly emphasise the striking duality of both formulations.

3.1. Spatial motion problem

The variation of the total energy $\mathscr{I}$ with respect to the spatial coordinates $\boldsymbol{X}$ at fixed material coordinates $\boldsymbol{X}$ can be expressed in the following form.

$$\delta_{\boldsymbol{x}}\mathscr{I} = \int_{\mathscr{B}_0} \nabla_{\boldsymbol{X}}\delta\bar{\boldsymbol{\varphi}} : \mathrm{D}_{\boldsymbol{F}}U_0 + \delta\bar{\boldsymbol{\varphi}}\cdot\partial_{\boldsymbol{x}}U_0\,\mathrm{d}V_0 = \int_{\mathscr{B}_t} \nabla_{\boldsymbol{x}}\delta\bar{\boldsymbol{\varphi}} : [U_t\boldsymbol{I} - \boldsymbol{f}^t\cdot\mathrm{d}_{\boldsymbol{f}}U_t] + \delta\bar{\boldsymbol{\varphi}}\cdot\partial_{\boldsymbol{x}}U_t\,\mathrm{d}V_t. \tag{23}$$

Hereby, we have made use of Eq. (9) for the variation of scalar-valued functions. Note that the push forward to the spatial domain given in the second line will be needed later on for the linearisation at fixed spatial coordinates. Thereby, the push forward of the first contribution is essentially based on the kinematic relation (18). The above format motivates the introduction of the spatial motion momentum fluxes $\boldsymbol{\Pi}^t$ and $\boldsymbol{\sigma}^t = j\boldsymbol{\Pi}^t\cdot\boldsymbol{F}^t$, whereby the former denotes the first Piola–Kirchhoff stress tensor while the latter is typically

referred to as Cauchy stress. Moreover, we introduce the corresponding momentum sources $\boldsymbol{b}_0$ and $\boldsymbol{b}_t$, i.e. the spatial volume force densities per unit volume in $\mathscr{B}_0$ and $\mathscr{B}_t$, respectively.

$$\begin{aligned} \boldsymbol{\Pi}^t &= \mathrm{D}_{\boldsymbol{F}} U_0 \quad \boldsymbol{b}_0 = -\partial_{\boldsymbol{x}} U_0, \\ \boldsymbol{\sigma}^t &= U_t \boldsymbol{I} - \boldsymbol{f}^t \cdot \mathrm{d}_f U_t \quad \boldsymbol{b}_t = -\partial_{\boldsymbol{x}} U_t. \end{aligned} \tag{24}$$

With the above definitions, the variation of the total energy (23) with respect to the spatial coordinates $\boldsymbol{x}$ takes the following more familiar format.

$$\delta_{\boldsymbol{x}} \mathscr{I} = \int_{\mathscr{B}_0} \nabla_{\boldsymbol{X}} \delta\bar{\boldsymbol{\varphi}} : \boldsymbol{\Pi}^t \, \mathrm{d}V_0 - \int_{\mathscr{B}_0} \delta\bar{\boldsymbol{\varphi}} \cdot \boldsymbol{b}_0 \, \mathrm{d}V_0 = \int_{\mathscr{B}_t} \nabla_x \delta\bar{\boldsymbol{\varphi}} : \boldsymbol{\sigma}^t \, \mathrm{d}V_t - \int_{\mathscr{B}_t} \delta\bar{\boldsymbol{\varphi}} : \boldsymbol{b}_t \, \mathrm{d}V_t. \tag{25}$$

According to the specific parametrisation of the internal and external potential energy density W_0 and V_0 introduced in Eq. (19), we obtain the following explicit representations for the spatial motion momentum fluxes and sources,

$$\begin{aligned} \boldsymbol{\Pi}^t &= \mathrm{D}_{\boldsymbol{F}} W_0 \quad \boldsymbol{b}_0 = -\partial_{\boldsymbol{x}} V_0, \\ \boldsymbol{\sigma}^t &= W_t \boldsymbol{I} - \boldsymbol{f}^t \cdot \mathrm{d}_f W_t \quad \boldsymbol{b}_t = -\partial_{\boldsymbol{x}} V_t \end{aligned} \tag{26}$$

by making use of the fact that $\mathrm{D}_{\boldsymbol{F}} V_0 \equiv \boldsymbol{0}$, $\partial_{\boldsymbol{x}} W_0 \equiv \boldsymbol{0}$ and $\mathrm{d}_f V_t \equiv V_t \boldsymbol{F}^t$. The specification of the internal potential energy density W_0 and the corresponding spatial motion momentum fluxes $\boldsymbol{\Pi}^t$ and $\boldsymbol{\sigma}^t$ for the particular case of a classical compressible Neo–Hooke material is given in the Appendix A.1.

3.2. Material motion problem

With the help of Eq. (9), the variation of total energy $\mathscr{I}$ with respect to the material coordinates $\boldsymbol{X}$ at fixed spatial coordinates $\boldsymbol{x}$ takes the following format.

$$\delta_{\boldsymbol{X}} \mathscr{I} = \int_{\mathscr{B}_t} \nabla_{\boldsymbol{x}} \delta\tilde{\boldsymbol{\Phi}} : \mathrm{d}_f U_t + \delta\tilde{\boldsymbol{\Phi}} \cdot \partial_{\boldsymbol{X}} U_t \, \mathrm{d}V_t = \int_{\mathscr{B}_0} \nabla_{\boldsymbol{X}} \delta\tilde{\boldsymbol{\Phi}} : [U_0 \boldsymbol{I} - \boldsymbol{F}^t \cdot \mathrm{D}_{\boldsymbol{F}} U_0] + \delta\tilde{\boldsymbol{\Phi}} \cdot \partial_{\boldsymbol{X}} U_0 \, \mathrm{d}V_0. \tag{27}$$

The pull back to the material domain expressed in the second line of the above equation will be needed later on for the linearisation at fixed material coordinates $\boldsymbol{X}$. In complete analogy to the spatial motion case, we can introduce the material motion momentum fluxes $\boldsymbol{\pi}^t$ and $\boldsymbol{\Sigma}^t$, a two-point stress tensor of Piola–Kirchhoff type and the classical Eshelby stress, respectively. Accordingly, the corresponding momentum sources, the material volume force densities per unit volume in $\mathscr{B}_t$ and $\mathscr{B}_0$, are introduced as $\boldsymbol{B}_t$ and $\boldsymbol{B}_0$.

$$\begin{aligned} \boldsymbol{\pi}^t &= \mathrm{d}_f U_t \quad \boldsymbol{B}_t = -\partial_{\boldsymbol{X}} U_t, \\ \boldsymbol{\Sigma}^t &= U_0 \boldsymbol{I} - \boldsymbol{F}^t \cdot \mathrm{D}_{\boldsymbol{F}} U_0 \quad \boldsymbol{B}_0 = -\partial_{\boldsymbol{X}} U_0. \end{aligned} \tag{28}$$

Consequently, the spatial variation of the total energy (27) can be reformulated in the following form.

$$\delta_{\boldsymbol{X}} \mathscr{I} = \int_{\mathscr{B}_t} \nabla_{\boldsymbol{x}} \delta\tilde{\boldsymbol{\Phi}} : \boldsymbol{\pi}^t \, \mathrm{d}V_t - \int_{\mathscr{B}_t} \delta\tilde{\boldsymbol{\Phi}} \cdot \boldsymbol{B}_t \, \mathrm{d}V_t = \int_{\mathscr{B}_0} \nabla_{\boldsymbol{X}} \delta\tilde{\boldsymbol{\Phi}} : \boldsymbol{\Sigma}^t \, \mathrm{d}V_0 - \int_{\mathscr{B}_0} \delta\tilde{\boldsymbol{\Phi}} \cdot \boldsymbol{B}_0 \, \mathrm{d}V_0. \tag{29}$$

By making use of the specific parametrisation of the internal and external potential energy introduced in Eq. (19), we can reformulate the momentum fluxes and sources.

$$\begin{aligned} \boldsymbol{\pi}^t &= \mathrm{d}_f W_t + V_t \boldsymbol{F}^t \quad \boldsymbol{B}_t = -\partial_{\boldsymbol{X}} W_t - \partial_{\boldsymbol{X}} V_t, \\ \boldsymbol{\Sigma}^t &= U_0 \boldsymbol{I} - \boldsymbol{F}^t \cdot \mathrm{D}_{\boldsymbol{F}} W_0 \quad \boldsymbol{B}_0 = -\partial_{\boldsymbol{X}} W_0 - \partial_{\boldsymbol{X}} V_0. \end{aligned} \tag{30}$$

Note that for the material motion problem, neither $\mathrm{d}_f V_t \neq \boldsymbol{0}$ nor $\partial_{\boldsymbol{X}} W_t \neq \boldsymbol{0}$ vanish identically. In the above expressions, we have made use of the identities $\mathrm{d}_f V_t = V_t \boldsymbol{F}^t$ and $\mathrm{D}_{\boldsymbol{F}} V_t = \boldsymbol{0}$, whereby the former accounts for contributions of possible volume forces. For the particular case of a classical compressible Neo–Hooke

material, the internal potential energy density W_t and the corresponding material motion momentum fluxes $\boldsymbol{\pi}^t$ and $\boldsymbol{\Sigma}^t$ are given in the Appendix A.2.

Remark 4 (*Spatial vs. material quantities*). In the continuous case, we can define the following relations between the spatial and material momentum fluxes.

$$\begin{aligned} \boldsymbol{\Pi}^t &= U_0 \boldsymbol{f}^t - J \boldsymbol{f}^t \cdot \boldsymbol{\pi}^t \cdot \boldsymbol{f}^t \quad \boldsymbol{\sigma}^t = U_t \boldsymbol{I} - \boldsymbol{f}^t \cdot \boldsymbol{\pi}^t, \\ \boldsymbol{\pi}^t &= U_t \boldsymbol{F}^t - j \boldsymbol{F}^t \cdot \boldsymbol{\Pi}^t \cdot \boldsymbol{F}^t \quad \boldsymbol{\Sigma}^t = U_0 \boldsymbol{I} - \boldsymbol{F}^t \cdot \boldsymbol{\Pi}^t. \end{aligned} \tag{31}$$

Remark 5 (*Spatial vs. material Euler–Lagrange equations*). The material and spatial variation of the total potential energy density suggest the spatial and the material version of the Euler–Lagrange field equations

$$\operatorname{div}_{\boldsymbol{X}}(\mathrm{D}_{\boldsymbol{F}} U_0) - \partial_{\boldsymbol{X}} U_0 = \boldsymbol{0} \quad \operatorname{div}_{\boldsymbol{X}}(\mathrm{d}_f U_t) - \partial_{\boldsymbol{X}} U_t = \boldsymbol{0}$$

which can be recast into the following more familiar statements

$$\operatorname{div}_{\boldsymbol{X}} \boldsymbol{\Pi}^t + \boldsymbol{b}_0 = \boldsymbol{0} \quad \operatorname{div}_{\boldsymbol{x}} \boldsymbol{\pi}^t + \boldsymbol{B}_t = \boldsymbol{0}$$

with the help of the definitions for the momentum fluxes and sources introduced in Eqs. (24) and (28). The former is typically referred to as the classical or spatial motion momentum balance while the latter corresponds to the material motion momentum balance also referred to as the balance of pseudomomentum. Recall that the former represents the balance of spatial forces, i.e. forces in the sense of Newton, while the latter corresponds to the balance of material forces, i.e. forces in the sense of Eshelby which are typically applied in defect mechanics.

4. Linearisation

The total variation of the overall potential energy $\delta\mathscr{I}$ renders the set of Euler–Lagrange field equations which represent a non-linear coupled system of equations in terms of the material and spatial coordinates. In what follows, we shall derive the total linearisation of this variational format, i.e. its linearisation at fixed referential coordinates $\boldsymbol{\xi}$.

$$\Delta\delta\mathscr{I} = \Delta[\delta_{\boldsymbol{x}}\mathscr{I}\,\delta_{\boldsymbol{X}}\mathscr{I}] = \Delta_{\boldsymbol{x}}\delta_{\boldsymbol{x}}\mathscr{I} + \Delta_{\boldsymbol{X}}\delta_{\boldsymbol{x}}\mathscr{I} + \Delta_{\boldsymbol{x}}\delta_{\boldsymbol{X}}\mathscr{I} + \Delta_{\boldsymbol{X}}\delta_{\boldsymbol{X}}\mathscr{I}. \tag{32}$$

Similar to the total variation, the total linearisation consists of the linearisation with respect to the spatial coordinates $\boldsymbol{x}$ at fixed material coordinates $\boldsymbol{X}$ plus the linearisation with respect to the material coordinates $\boldsymbol{X}$ at fixed spatial coordinates $\boldsymbol{x}$ which will be elaborated in detail in the sequel.

4.1. Spatial motion problem

Let us first consider the linearisation of spatial motion problem $\delta_{\boldsymbol{x}}\mathscr{I}$ with respect to $\boldsymbol{x}$ at fixed material coordinates $\boldsymbol{X}$ which follows from the linearisation of the first line of Eq. (23) defined over the material domain $\mathscr{B}_0$.

$$\Delta_{\boldsymbol{x}}\delta_{\boldsymbol{x}}\mathscr{I} = \int_{\mathscr{B}_0} \nabla_{\boldsymbol{X}}\delta\bar{\boldsymbol{\varphi}} : [\mathrm{D}^2_{\boldsymbol{FF}} U_0 : \nabla_{\boldsymbol{X}}\Delta\bar{\boldsymbol{\varphi}} + \partial_{\boldsymbol{x}}\mathrm{D}_{\boldsymbol{F}} U_0 \cdot \Delta\bar{\boldsymbol{\varphi}}] + \delta\bar{\boldsymbol{\varphi}} \cdot [\mathrm{D}_{\boldsymbol{F}}\partial_{\boldsymbol{x}} U_0 : \nabla_{\boldsymbol{X}}\Delta\bar{\boldsymbol{\varphi}} + \partial^2_{\boldsymbol{xx}} U_0 \cdot \Delta\bar{\boldsymbol{\varphi}}]\,\mathrm{d}V_0. \tag{33}$$

For the particular parametrisation chosen in (19), the first term $\mathrm{D}^2_{\boldsymbol{FF}} U_0 = \mathrm{D}^2_{\boldsymbol{FF}} W_0$ represents the classical tangent operator, the second and third term $\mathrm{D}_{\boldsymbol{F}}\partial_{\boldsymbol{x}} U_0 = \partial_{\boldsymbol{x}}\mathrm{D}_{\boldsymbol{F}} U_0 = \boldsymbol{0}$ vanish identically and the fourth term

$\partial^2_{\boldsymbol{xx}} U_0 = \partial^2_{\boldsymbol{xx}} V_0$ accounts for deformation dependent loading if V_0 is a non-linear function in $\boldsymbol{x}$. In what follows, we shall assume the particular case with $V_0 = -\boldsymbol{b}_0 \cdot \boldsymbol{\varphi}$ with $\boldsymbol{b}_0 = \text{const.}$ such that $\partial^2_{\boldsymbol{xx}} V_0 = \boldsymbol{0}$. The linearisation of spatial motion problem with respect to the material coordinates $\boldsymbol{X}$ at fixed spatial coordinates $\boldsymbol{x}$ follows from the second line of Eq. (23) defined over the spatial domain $\mathscr{B}_t$.

$$\begin{aligned} \Delta_{\boldsymbol{X}} \delta_{\boldsymbol{x}} \mathscr{I} = & \int_{\mathscr{B}_t} \nabla_{\boldsymbol{x}} \delta\bar{\boldsymbol{\varphi}} : [\boldsymbol{I} \otimes \mathrm{d}_f U_t - \boldsymbol{I} \underline{\otimes} [\mathrm{d}_f U_t]^t - \boldsymbol{f}^t \cdot \mathrm{d}^2_{ff} U_t] : \nabla_{\boldsymbol{x}} \Delta\tilde{\boldsymbol{\Phi}} \\ & + \nabla_{\boldsymbol{x}} \delta\bar{\boldsymbol{\varphi}} : [\boldsymbol{I} \otimes \partial_{\boldsymbol{X}} U_t - \boldsymbol{f}^t \cdot \partial_{\boldsymbol{X}} \mathrm{d}_f U_t] \cdot \Delta\tilde{\boldsymbol{\Phi}} + \delta\bar{\boldsymbol{\varphi}} \cdot [\mathrm{d}_f \partial_{\boldsymbol{x}} U_t : \nabla_{\boldsymbol{x}} \Delta\tilde{\boldsymbol{\Phi}} + \partial_{\boldsymbol{X}} \partial_{\boldsymbol{x}} U_t \cdot \Delta\tilde{\boldsymbol{\Phi}}] \, \mathrm{d}V_t. \end{aligned} \tag{34}$$

In particular, for the problems considered later on with the parametrisation suggested in (19) and with the assumption of material homogeneity and thus no explicit dependence on the material coordinate $\boldsymbol{X}$ such that $\partial_{\boldsymbol{X}} U_t = \boldsymbol{0}$ the above linearisations reduce to the following expressions.

$$\begin{aligned} \Delta_{\boldsymbol{x}} \delta_{\boldsymbol{x}} \mathscr{I} &= \int_{\mathscr{B}_0} \nabla_{\boldsymbol{X}} \delta\bar{\boldsymbol{\varphi}} : \mathbf{A} : \nabla_{\boldsymbol{X}} \Delta\bar{\boldsymbol{\varphi}} \, \mathrm{d}V_0 = \int_{\mathscr{B}_0} \nabla_{\boldsymbol{x}} \delta\bar{\boldsymbol{\varphi}} : \mathbf{c} : \nabla_{\boldsymbol{x}} \Delta\bar{\boldsymbol{\varphi}} \, \mathrm{d}V_0, \\ \Delta_{\boldsymbol{X}} \delta_{\boldsymbol{x}} \mathscr{I} &= \int_{\mathscr{B}_t} \nabla_{\boldsymbol{x}} \delta\bar{\boldsymbol{\varphi}} : \mathrm{d}_f \boldsymbol{\sigma}^t : \nabla_{\boldsymbol{x}} \Delta\tilde{\boldsymbol{\Phi}} \, \mathrm{d}V_t - \int_{\mathscr{B}_t} \delta\bar{\boldsymbol{\varphi}} \cdot \boldsymbol{b}_t \otimes \boldsymbol{F} : \nabla_{\boldsymbol{x}} \Delta\tilde{\boldsymbol{\Phi}} \, \mathrm{d}V_t. \end{aligned} \tag{35}$$

Hereby, we have made use of the definitions (28) with $\boldsymbol{\pi}^t = \mathrm{d}_f U_t$ and $\boldsymbol{b}_t = -\partial_{\boldsymbol{x}} U_t$ and the abbreviations

$$\begin{aligned} &\mathbf{A} = \mathrm{D}^2_{\boldsymbol{FF}} U_0 = \mathrm{D}_{\boldsymbol{F}} \boldsymbol{\Pi}^t \quad \mathbf{c} = [\boldsymbol{I} \overline{\otimes} \boldsymbol{F}] : \mathbf{A} : [\boldsymbol{I} \overline{\otimes} \boldsymbol{F}^t], \\ &\mathrm{d}_f \boldsymbol{\sigma}^t = \boldsymbol{I} \otimes \boldsymbol{\pi}^t - \boldsymbol{I} \underline{\otimes} \boldsymbol{\pi} - \mathbf{g} \quad \mathbf{g} = [\boldsymbol{f}^t \overline{\otimes} \boldsymbol{I}] : \mathbf{a} : [\boldsymbol{I} \overline{\otimes} \boldsymbol{I}], \end{aligned} \tag{36}$$

whereby the component representation of the non-standard dyadic products reads $\{\bullet \overline{\otimes} \circ\}_{ijkl} = \{\bullet\}_{ik} \otimes \{\circ\}_{jl}$ and $\{\bullet \underline{\otimes} \circ\}_{ijkl} = \{\bullet\}_{il} \otimes \{\circ\}_{jk}$. The fourth order operator $\mathbf{g}$ is defined in terms of the material motion tangent operator $\mathbf{a}$ to be introduced in the next subsection. The specification of the individual tangent operators $\mathbf{A}$, $\mathbf{c}$ and $\mathbf{g}$ for a classical compressible Neo–Hooke material is given in the Appendix A.

4.2. Material motion problem

The linearisation of the material motion problem $\delta_{\boldsymbol{X}} \mathscr{I}$ with respect to the material coordinates $\boldsymbol{X}$ at fixed spatial coordinates $\boldsymbol{x}$ follows from the first row of Eq. (27) which is defined over the spatial domain $\mathscr{B}_t$.

$$\Delta_{\boldsymbol{X}} \delta_{\boldsymbol{X}} \mathscr{I} = \int_{\mathscr{B}_t} \nabla_{\boldsymbol{x}} \delta\tilde{\boldsymbol{\Phi}} : [\mathrm{d}^2_{ff} U_t : \nabla_{\boldsymbol{x}} \Delta\tilde{\boldsymbol{\Phi}} + \partial_{\boldsymbol{X}} \mathrm{d}_f U_t \cdot \Delta\tilde{\boldsymbol{\Phi}}] + \delta\tilde{\boldsymbol{\Phi}} \cdot [\mathrm{d}_f \partial_{\boldsymbol{X}} U_t : \nabla_{\boldsymbol{x}} \Delta\tilde{\boldsymbol{\Phi}} + \partial^2_{\boldsymbol{XX}} U_t \cdot \Delta\tilde{\boldsymbol{\Phi}}] \, \mathrm{d}V_t. \tag{37}$$

Herein, the first term $\mathrm{d}^2_{ff} U_t$ constitutes the material motion tangent operator. In the materially homogeneous case considered later on, the second, third and fourth term vanish identically since $\partial_{\boldsymbol{X}} U_t = \boldsymbol{0}$. For the linearisation of the material motion problem with respect to the spatial coordinates $\boldsymbol{x}$ at fixed material coordinates $\boldsymbol{X}$ we make use of the second line of Eq. (27) defined over the material domain $\mathscr{B}_0$. It renders the following expression.

$$\begin{aligned} \Delta_{\boldsymbol{x}} \delta_{\boldsymbol{X}} \mathscr{I} = & \int_{\mathscr{B}_0} \nabla_{\boldsymbol{X}} \delta\tilde{\boldsymbol{\Phi}} : [\boldsymbol{I} \otimes \mathrm{D}_{\boldsymbol{F}} U_0 - \boldsymbol{I} \underline{\otimes} [\mathrm{D}_{\boldsymbol{F}} U_0]^t - \boldsymbol{F}^t \cdot \mathrm{D}^2_{\boldsymbol{FF}} U_0] : \nabla_{\boldsymbol{X}} \Delta\bar{\boldsymbol{\varphi}} \\ & + \nabla_{\boldsymbol{X}} \delta\tilde{\boldsymbol{\Phi}} : [\boldsymbol{I} \otimes \partial_{\boldsymbol{x}} U_0 - \boldsymbol{F}^t \cdot \partial_{\boldsymbol{x}} \mathrm{D}_{\boldsymbol{F}} U_0] \cdot \Delta\bar{\boldsymbol{\varphi}} + \delta\tilde{\boldsymbol{\Phi}} \cdot [\mathrm{D}_{\boldsymbol{F}} \partial_{\boldsymbol{X}} U_0 : \nabla_{\boldsymbol{X}} \Delta\bar{\boldsymbol{\varphi}} + \partial_{\boldsymbol{x}} \partial_{\boldsymbol{X}} U_0 \cdot \Delta\bar{\boldsymbol{\varphi}}] \, \mathrm{d}V_0. \end{aligned} \tag{38}$$

Recall that for the materially homogeneous case to be considered in the sequel, the last two terms vanish identically since $\partial_{\boldsymbol{X}} U_0 = \boldsymbol{0}$. Moreover, as $\partial_{\boldsymbol{x}} \mathrm{D}_{\boldsymbol{F}} U_0 = \partial_{\boldsymbol{x}} \boldsymbol{\Pi}^t = \boldsymbol{0}$ the fifth term vanishes as well. Consequently, the above linearisations thus reduce to the following expressions

$$\begin{aligned}
\Delta_{\boldsymbol{X}}\delta_{\boldsymbol{X}}\mathscr{I} &= \int_{\mathscr{B}_t} \nabla_{\boldsymbol{x}}\delta\tilde{\boldsymbol{\Phi}} : \mathbf{a} : \nabla_{\boldsymbol{x}}\Delta\tilde{\boldsymbol{\Phi}}\,\mathrm{d}V_t = \int_{\mathscr{B}_t} \nabla_{\boldsymbol{X}}\delta\tilde{\boldsymbol{\Phi}} : \mathbf{C} : \nabla_{\boldsymbol{X}}\Delta\tilde{\boldsymbol{\Phi}}\,\mathrm{d}V_t, \\
\Delta_{\boldsymbol{x}}\delta_{\boldsymbol{X}}\mathscr{I} &= \int_{\mathscr{B}_0} \nabla_{\boldsymbol{X}}\delta\tilde{\boldsymbol{\Phi}} : \mathrm{D}_{\boldsymbol{F}}\boldsymbol{\Sigma}^t : \nabla_{\boldsymbol{X}}\Delta\bar{\boldsymbol{\varphi}}\,\mathrm{d}V_0 - \int_{\mathscr{B}_0} \nabla_{\boldsymbol{X}}\delta\tilde{\boldsymbol{\Phi}} : \boldsymbol{I}\otimes\boldsymbol{b}_0\cdot\Delta\bar{\boldsymbol{\varphi}}\,\mathrm{d}V_0
\end{aligned} \tag{39}$$

with the definitions $\boldsymbol{\Pi}^t = \mathrm{D}_{\boldsymbol{F}}U_0$ and $\boldsymbol{b}_0 = -\partial_{\boldsymbol{x}}U_0$ according to Eq. (24) and the abbreviations

$$\begin{aligned}
&\mathbf{a} = \mathrm{d}^2_{\boldsymbol{ff}}U_t = \mathrm{d}_{\boldsymbol{f}}\boldsymbol{\pi}^t \quad \mathbf{C} = [\boldsymbol{I}\overline{\otimes}\boldsymbol{f}] : \mathbf{a} : [\boldsymbol{I}\overline{\otimes}\boldsymbol{f}^t], \\
&\mathrm{D}_{\boldsymbol{F}}\boldsymbol{\Sigma}^t = \boldsymbol{I}\otimes\boldsymbol{\Pi}^t - \boldsymbol{I}\underline{\otimes}\boldsymbol{\Pi} - \mathbf{G} \quad \mathbf{G} = [\boldsymbol{F}^t\overline{\otimes}\boldsymbol{I}] : \mathbf{A} : [\boldsymbol{I}\overline{\otimes}\boldsymbol{I}],
\end{aligned} \tag{40}$$

whereby the fourth order operator $\mathbf{G}$ is defined in terms of the spatial motion tangent operator $\mathbf{A}$ which was introduced in the previous subsection in equation (36). The specification of the individual tangent operators $\mathbf{a}$, $\mathbf{C}$ and $\mathbf{G}$ for the particular case of a classical compressible Neo–Hooke material is given in the Appendix A.

Remark 6 (*Symmetry*). Since the present ALE formulation is derived from a potential, the variational ALE technique is symmetric in the sense that $\Delta_{\boldsymbol{X}}\delta_{\boldsymbol{x}}\mathscr{I}$ correlates with $\Delta_{\boldsymbol{x}}\delta_{\boldsymbol{X}}\mathscr{I}$. Symmetry is not visible explicitly when comparing Eqs. (34) and (38), because the main focus of the present contribution was the aspect of duality. The issue of symmetry will be elaborated in detail in Part 2 of this paper, see Askes et al. [40]. The symmetry property is particularly appealing in the context of the finite element formulation which will be derived in the next section since it carries over to symmetric system matrices upon discretisation.

5. Discretisation

In the spirit of the finite element method, the reference domain $\mathscr{B}_\square$ is discretised in n_{el} elements which are characterised through the corresponding element domain $\mathscr{B}^e_\square$. The underlying geometry $\boldsymbol{\xi}$ is interpolated elementwise by the shape functions N^i_{ξ} in terms of the discrete node point positions $\boldsymbol{\xi}_i$ of the $i = 1,\ldots,n_{en}$ element nodes.

$$\mathscr{B}_\square = \bigcup_{e=1}^{n_{\mathrm{el}}} \mathscr{B}^e_\square \quad \boldsymbol{\xi}^h|_{\mathscr{B}^e_\square} = \sum_{i=1}^{n_{en}} N^i_{\xi}\boldsymbol{\xi}_i. \tag{41}$$

Following the isoparametric concept, the unknowns $\bar{\boldsymbol{\varphi}}$ and $\tilde{\boldsymbol{\Phi}}$ are interpolated on the element level with the same shape functions $N^i_{\bar{\varphi}}$ and $N^j_{\tilde{\Phi}}$ as the element geometry $\boldsymbol{\xi}$. Similar shape functions are applied to interpolate the test functions $\delta\bar{\boldsymbol{\varphi}}$ and $\delta\tilde{\boldsymbol{\Phi}}$ according to the classical Bubnov–Galerkin technique.

$$\begin{aligned}
&\delta\bar{\boldsymbol{\varphi}}^h|_{\mathscr{B}^e_\square} = \sum_{i=1}^{n_{en}} N^i_{\bar{\varphi}}\delta\bar{\boldsymbol{\varphi}}_i \in H^0_1(\mathscr{B}_\square) \quad \bar{\boldsymbol{\varphi}}^h|_{\mathscr{B}^e_\square} = \sum_{k=1}^{n_{en}} N^k_{\bar{\varphi}}\bar{\boldsymbol{\varphi}}_k D \in H_1(\mathscr{B}_\square), \\
&\delta\tilde{\boldsymbol{\Phi}}^h|_{\mathscr{B}^e_\square} = \sum_{j=1}^{n_{en}} N^j_{\tilde{\Phi}}\delta\tilde{\boldsymbol{\Phi}}_j \in H^0_1(\mathscr{B}_\square) \quad \tilde{\boldsymbol{\Phi}}^h|_{\mathscr{B}^e_\square} = \sum_{l=1}^{n_{en}} N^l_{\tilde{\Phi}}\tilde{\boldsymbol{\Phi}}_l \in H_1(\mathscr{B}_\square).
\end{aligned} \tag{42}$$

Consequently, the related gradients of the test functions $\nabla_{\xi}\delta\bar{\boldsymbol{\varphi}}^h$ and $\nabla_{\xi}\delta\tilde{\boldsymbol{\Phi}}^h$ and the gradients of the primary unknowns $\nabla_{\xi}\bar{\boldsymbol{\varphi}}^h$ and $\nabla_{\xi}\tilde{\boldsymbol{\Phi}}^h$ take the following elementwise interpolation.

$$\begin{aligned}
\nabla_\xi \delta\bar{\boldsymbol{\varphi}}^h|_{\mathscr{B}^e_\square} &= \sum_{i=1}^{n_{en}} \delta\bar{\boldsymbol{\varphi}}_i \otimes \nabla_\xi N^i_{\bar{\varphi}} \quad \nabla_\xi \bar{\boldsymbol{\varphi}}^h|_{\mathscr{B}^e_\square} = \sum_{k=1}^{n_{en}} \bar{\boldsymbol{\varphi}}_k \otimes \nabla_\xi N^k_{\bar{\varphi}}, \\
\nabla_\xi \delta\tilde{\boldsymbol{\Phi}}^h|_{\mathscr{B}^e_\square} &= \sum_{j=1}^{n_{en}} \delta\tilde{\boldsymbol{\Phi}}_j \otimes \nabla_\xi N^j_{\tilde{\Phi}} \quad \nabla_\xi \tilde{\boldsymbol{\Phi}}^h|_{\mathscr{B}^e_\square} = \sum_{l=1}^{n_{en}} \tilde{\boldsymbol{\Phi}}_l \otimes \nabla_\xi N^l_{\tilde{\Phi}}.
\end{aligned} \tag{43}$$

In particular, $\nabla_\xi \bar{\boldsymbol{\varphi}}^h$ and $\nabla_\xi \tilde{\boldsymbol{\Phi}}^h$ denote the discrete deformation gradients $\bar{\boldsymbol{F}}^h = \nabla_\xi \bar{\boldsymbol{\varphi}}^h$ and $\tilde{\boldsymbol{f}}^h = \nabla_\xi \tilde{\boldsymbol{\Phi}}^h$, which define the discrete spatial and material deformation gradient as $\boldsymbol{F}^h = \bar{\boldsymbol{F}}^h \cdot \tilde{\boldsymbol{F}}^h$ and $\boldsymbol{f}^h = \tilde{\boldsymbol{f}}^h \cdot \bar{\boldsymbol{f}}^h$. With the above suggested discretisations at hand, the discrete residual of the balance of momentum of the spatial motion problem $\mathbf{R}^I_{\bar{\varphi}}$ and of the material motion problem $\mathbf{R}^J_{\tilde{\Phi}}$ can be expressed $\forall I, J = 1, \ldots, n_{np}$ as

$$\begin{aligned}
\mathbf{R}^I_{\bar{\varphi}}(\bar{\boldsymbol{\varphi}}^h, \tilde{\boldsymbol{\Phi}}^h) &= \mathop{\mathbf{A}}_{e=1}^{n_{\mathrm{el}}} \int_{\mathscr{B}^e_t} \nabla_{\boldsymbol{x}} N^i_{\bar{\varphi}} \cdot \boldsymbol{\sigma}\, \mathrm{d}V_t - \int_{\partial\mathscr{B}^{te}_t} N^i_{\bar{\varphi}} \boldsymbol{t}_t\, \mathrm{d}A_t - \int_{\mathscr{B}^e_t} N^i_{\bar{\varphi}} \boldsymbol{b}_t\, \mathrm{d}V_t = \mathbf{0}, \\
\mathbf{R}^J_{\tilde{\Phi}}(\bar{\boldsymbol{\varphi}}^h, \tilde{\boldsymbol{\Phi}}^h) &= \mathop{\mathbf{A}}_{e=1}^{n_{\mathrm{el}}} \int_{\mathscr{B}^e_0} \nabla_{\boldsymbol{X}} N^j_{\tilde{\Phi}} \cdot \boldsymbol{\Sigma}\, \mathrm{d}V_0 - \int_{\partial\mathscr{B}^{te}_0} N^j_{\tilde{\Phi}} \boldsymbol{T}_0\, \mathrm{d}A_0 - \int_{\mathscr{B}^e_0} N^j_{\tilde{\Phi}} \boldsymbol{b}_0\, \mathrm{d}V_0 = \mathbf{0}
\end{aligned} \tag{44}$$

with the understanding that the operator $\mathbf{A}_{e=1}^{n_{\mathrm{el}}}$ denotes the assembly over all $e = 1, \ldots, n_{\mathrm{el}}$ element contributions at the $i, j = 1, \ldots, n_{en}$ element nodes to the global node point residuals at all $I, J = 1, \ldots, n_{np}$ global node points. The above derived discrete residual statements represent a highly non-linear coupled system of equations which can be solved efficiently within the framework of a monolithic incremental iterative Newton–Raphson solution strategy. To this end, we perform a consistent linearisation of the governing equations

$$\begin{aligned}
\mathbf{R}^{Ik+1}_{\bar{\varphi}} &= \mathbf{R}^{Ik}_{\bar{\varphi}} + \mathrm{d}\mathbf{R}^I_{\bar{\varphi}} \doteq \mathbf{0} \quad \mathrm{d}\mathbf{R}^I_{\bar{\varphi}} = \sum_{K=1}^{n_{np}} \mathbf{K}^{IK}_{\bar{\varphi}\bar{\varphi}} \mathrm{d}\bar{\boldsymbol{\varphi}}_K + \sum_{L=1}^{n_{np}} \mathbf{K}^{IL}_{\bar{\varphi}\tilde{\Phi}} \cdot \mathrm{d}\tilde{\boldsymbol{\Phi}}_L, \\
\mathbf{R}^{Jk+1}_{\tilde{\Phi}} &= \mathbf{R}^{Jk}_{\tilde{\Phi}} + \mathrm{d}\mathbf{R}^J_{\tilde{\Phi}} \doteq \mathbf{0} \quad \mathrm{d}\mathbf{R}^J_{\tilde{\Phi}} = \sum_{K=1}^{n_{np}} \mathbf{K}^{JK}_{\tilde{\Phi}\bar{\varphi}} \mathrm{d}\bar{\boldsymbol{\varphi}}_K + \sum_{L=1}^{n_{np}} \mathbf{K}^{JL}_{\tilde{\Phi}\tilde{\Phi}} \cdot \mathrm{d}\tilde{\boldsymbol{\Phi}}_L
\end{aligned} \tag{45}$$

with $\mathrm{d}\mathbf{R}^I_{\bar{\varphi}}$ and $\mathrm{d}\mathbf{R}^J_{\tilde{\Phi}}$ denoting the iterative residual of the iteration $k+1$. The iteration matrices $\mathbf{K}^{IK}_{\bar{\varphi}\bar{\varphi}}$, $\mathbf{K}^{IL}_{\bar{\varphi}\tilde{\Phi}}$, $\mathbf{K}^{JK}_{\tilde{\Phi}\bar{\varphi}}$ and $\mathbf{K}^{JL}_{\tilde{\Phi}\tilde{\Phi}}$ can finally be expressed as

$$\begin{aligned}
\mathbf{K}^{IK}_{\bar{\varphi}\bar{\varphi}} &= \frac{\partial \mathbf{R}^I_{\bar{\varphi}}}{\partial \bar{\boldsymbol{\varphi}}_K} = \mathop{\mathbf{A}}_{e=1}^{n_{\mathrm{el}}} \int_{\mathscr{B}^e_0} \nabla_{\boldsymbol{x}} N^i_{\bar{\varphi}} \cdot \mathbf{c} \cdot \nabla_{\boldsymbol{x}} N^k_{\bar{\varphi}}\, \mathrm{d}V_0, \\
\mathbf{K}^{IL}_{\bar{\varphi}\tilde{\Phi}} &= \frac{\partial \mathbf{R}^I_{\bar{\varphi}}}{\partial \tilde{\boldsymbol{\Phi}}_L} = \mathop{\mathbf{A}}_{e=1}^{n_{\mathrm{el}}} \int_{\mathscr{B}^e_t} \nabla_{\boldsymbol{x}} N^i_{\bar{\varphi}} \cdot \mathrm{d}_{\boldsymbol{f}} \boldsymbol{\sigma}^t \cdot \nabla_{\boldsymbol{x}} N^l_{\tilde{\Phi}}\, \mathrm{d}V_t - \int_{\mathscr{B}^e_t} N^i_{\bar{\varphi}} \boldsymbol{b}_t \cdot \nabla_{\boldsymbol{X}} N^l_{\tilde{\Phi}}\, \mathrm{d}V_t, \\
\mathbf{K}^{JK}_{\tilde{\Phi}\bar{\varphi}} &= \frac{\partial \mathbf{R}^J_{\tilde{\Phi}}}{\partial \bar{\boldsymbol{\varphi}}_K} = \mathop{\mathbf{A}}_{e=1}^{n_{\mathrm{el}}} \int_{\mathscr{B}^e_0} \nabla_{\boldsymbol{X}} N^j_{\tilde{\Phi}} \cdot \mathrm{D}_{\boldsymbol{F}} \boldsymbol{\Sigma}^t \cdot \nabla_{\boldsymbol{X}} N^k_{\bar{\varphi}}\, \mathrm{d}V_0 - \int_{\mathscr{B}^e_0} \nabla_{\boldsymbol{X}} N^j_{\tilde{\Phi}} \cdot \boldsymbol{b}_0 N^k_{\bar{\varphi}}\, \mathrm{d}V_0, \\
\mathbf{K}^{JL}_{\tilde{\Phi}\tilde{\Phi}} &= \frac{\partial \mathbf{R}^J_{\tilde{\Phi}}}{\partial \tilde{\boldsymbol{\Phi}}_L} = \mathop{\mathbf{A}}_{e=1}^{n_{\mathrm{el}}} \int_{\mathscr{B}^e_t} \nabla_{\boldsymbol{X}} N^j_{\tilde{\Phi}} \cdot \mathbf{C} \cdot \nabla_{\boldsymbol{X}} N^l_{\tilde{\Phi}}\, \mathrm{d}V_t
\end{aligned} \tag{46}$$

in terms of the fourth order tensors $\mathbf{C}$, $\mathrm{d}_{\boldsymbol{f}}\boldsymbol{\sigma}^t$, $\mathrm{D}_{\boldsymbol{F}}\boldsymbol{\Sigma}^t$ and $\mathbf{C}$ according to the definitions (36) and (40) derived earlier in Section 4. The solution of the system of Eqs. (45) renders the iterative update for the global unknowns $\bar{\boldsymbol{\varphi}}_I$ and $\tilde{\boldsymbol{\Phi}}_J$.

$$\bar{\boldsymbol{\varphi}}_I = \bar{\boldsymbol{\varphi}}_I + \mathrm{d}\bar{\boldsymbol{\varphi}}_I \quad \tilde{\boldsymbol{\Phi}}_J = \tilde{\boldsymbol{\Phi}}_J + \mathrm{d}\tilde{\boldsymbol{\Phi}}_J. \tag{47}$$

Remark 7 (*Spatial vs. material quantities*). It is important to recognise that the relations between spatial and material quantities derived in the previous sections are valid only for the continuous case. Upon discretisation, we introduce the spatial and the material motion problem as independent statements. In particular, a vanishing residual $\mathbf{R}^I_{\bar{\varphi}}$ of the spatial motion problem does not necessarily have to correspond to a vanishing residual $\mathbf{R}^J_{\tilde{\Phi}}$ of the material motion problem and vice versa, see Askes et al. [40].

Remark 8 (*Spatial vs. material forces*). The discrete residual $\mathbf{R}^I_{\bar{\varphi}}$ and $\mathbf{R}^J_{\tilde{\Phi}}$ introduced in Eq. (44) define the discrete spatial and material surface forces $\mathbf{f}^{Ih}_{\varphi\text{sur}}$ and $\mathbf{F}^{Jh}_{\Phi\text{sur}}$,

$$\begin{aligned}\mathbf{f}^{Ih}_{\varphi\text{sur}} &= \mathop{\mathsf{A}}_{e=1}^{n_{\text{el}}} \int_{\mathscr{B}^e_t} \nabla_{\boldsymbol{x}} N^i_{\bar{\varphi}} \cdot \boldsymbol{\sigma} - N^i_{\bar{\varphi}} \boldsymbol{b}_t \, \mathrm{d}V_t, \\ \mathbf{F}^{Jh}_{\Phi\text{sur}} &= \mathop{\mathsf{A}}_{e=1}^{n_{\text{el}}} \int_{\mathscr{B}^e_0} \nabla_{\boldsymbol{X}} N^j_{\tilde{\Phi}} \cdot \boldsymbol{\Sigma} - N^j_{\tilde{\Phi}} \boldsymbol{B}_0 \, \mathrm{d}V_0\end{aligned} \tag{48}$$

which are energetically conjugated to the spatial variations $\delta\bar{\boldsymbol{\varphi}}_I$ and to the material variations $\delta\tilde{\boldsymbol{\Phi}}_J$ of the node point positions. Recall that material forces $\mathbf{F}^{Jh}_{\Phi\text{sur}}$ are typically associated with positional changes of defects, e.g. the motion of dislocations or the opening of a crack. In the context considered herein, the finite element discretisation can thus be interpreted as a source of inhomogeneity introducing discrete defects.

Remark 9 (*Lagrangian vs. Eulerian viewpoint*). The classical Lagrangian and Eulerian viewpoint can be derived as special cases with keeping either $\tilde{\boldsymbol{\Phi}}$ or $\bar{\boldsymbol{\varphi}}$ fixed such that either $\bar{\boldsymbol{\varphi}} = \bar{\boldsymbol{\varphi}}$ or $\boldsymbol{\Phi} = \tilde{\boldsymbol{\Phi}}$. In the first case corresponding the Lagrangian viewpoint, the $\tilde{\boldsymbol{\Phi}}$ terms in Eqs. (44) and (46) would vanish identically as $\mathbf{R}^J_{\tilde{\Phi}} = \mathbf{0}$, $\mathbf{K}^{IL}_{\bar{\varphi}\tilde{\Phi}} = \mathbf{0}$, $\mathbf{K}^{JK}_{\tilde{\Phi}\bar{\varphi}} = \mathbf{0}$ and $\mathbf{K}^{JL}_{\tilde{\Phi}\tilde{\Phi}} = \mathbf{0}$ while for the second case corresponding to the Eulerian viewpoint the $\bar{\boldsymbol{\varphi}}$ terms would vanish such that $\mathbf{R}^I_{\bar{\varphi}} = \mathbf{0}$, $\mathbf{K}^{IK}_{\bar{\varphi}\bar{\varphi}} = \mathbf{0}$, $\mathbf{K}^{IL}_{\bar{\varphi}\tilde{\Phi}} = \mathbf{0}$ and $\mathbf{K}^{JK}_{\tilde{\Phi}\bar{\varphi}} = \mathbf{0}$.

Remark 10 (*Monolithic vs. staggered solution*). Note that the formulation derived herein suggests a monolithic solution for the spatial and the material node point positions. However, a staggered solution scheme can be derived from the proposed algorithm in a straightforward way. It essentially follows from the above-derived equations by neglecting the coupling matrices $\mathbf{K}^{IL}_{\bar{\varphi}\tilde{\Phi}} = \mathbf{0}$ and $\mathbf{K}^{JK}_{\tilde{\Phi}\bar{\varphi}} = \mathbf{0}$ such that the spatial and the material motion problem can be solved individually. A detailed comparison between monolithic and staggered schemes is given in Part 2 of this contribution, see Askes et al. [40].

6. Discussion

The main idea of the present contribution was the derivation of an Arbitrary Lagrangian–Eulerian formulation which is embedded in a consistent variational framework. Being essentially characterised through a spatial and a material mapping, the formulation is inherently related to the mechanics on the spatial and the material manifold. The governing equations follow straightforwardly from the evaluation of the corresponding ALE Dirichlet principle based on the total variation of the overall potential energy. By reformulating this total variation with respect to fixed reference coordinates as the sum of the variation with respect to the spatial coordinates at fixed material positions plus the variation with respect to the material coordinates at fixed spatial position, we obtained the Euler–Lagrange equations of the ALE formulation, i.e. the spatial and the material motion version of the balance of linear momentum. The solution of the former renders the spatial configuration while the latter defines the related material configuration and thus the optimal node point positions of the underlying mesh which minimises the overall potential energy.

The Euler–Lagrange equations can be interpreted as spatial and material force balance, respectively. In the continuous hyperelastic case, both statements are entirely equivalent for homogeneous problems.

However, this equivalence is no longer valid upon discretisation, i.e. a vanishing discrete spatial forces do not necessarily have to coincide with vanishing discrete material forces and vice versa. Paralleling the traditional application, where continuous material forces are used to investigate material inhomogeneities, discrete material forces can be used to detect numerical inhomogeneities induced by the underlying finite element discretisation. An additional release of energy can be observed when moving nodes of the finite element mesh in the direction opposite to the material force acting on it. An optimal mesh thus corresponds to vanishing discrete material node point forces. In this sense, the remeshing strategy is no longer user-defined but objective with respect to energy minimisation.

Based on arguments of duality, our formulation is essentially characterised through the discretisation and simultaneous solution of both, the spatial and the material motion problem. In this sense, the variational ALE framework is particularly appealing since it renders symmetric system matrices upon discretisation. The presented generic framework is therefore considered as an elegant and powerful strategy to derive optimal meshes on a consistent variational basis. Its application to Neo–Hookean hyperelasticity and particular details concerning its numerical realisation will be elaborated in Part 2 of this contribution.

Appendix A. Model problem: compressible Neo–Hooke material

In this appendix, we specify the constitutive equations for the model problem of a classical compressible Neo–Hooke material. For the sake of clarity, we shall restrict ourselves to the specification of the contributions originating from the internal potential energy $W_{\square}$.

A.1. Spatial motion problem

The internal potential energy $W_0(\boldsymbol{F})$ of the spatial motion problem

$$W_0 = \tfrac{1}{2}\lambda_0 \ln^2 J + \tfrac{1}{2}\mu_0[\boldsymbol{F} : \boldsymbol{F}^t - n^{\dim} - 2\ln J] \tag{A.1}$$

can be expressed in terms of the spatial motion deformation gradient $\boldsymbol{F}$ and its Jacobian J and the corresponding Lamé constants λ_0 and μ_0, whereby $n^{\dim}$ denotes the number of spatial dimensions. The internal potential energy basically defines the spatial motion momentum fluxes, i.e. the first Piola–Kirchhoff stress tensor $\boldsymbol{\Pi}^t = \mathrm{D}_{\boldsymbol{F}} W_0$ and the Cauchy stress tensor $\boldsymbol{\sigma}^t = j\boldsymbol{\Pi}^t \cdot \boldsymbol{F}^t$ which take the following explicit expressions.

$$\begin{aligned} \boldsymbol{\Pi}^t &= [\lambda_0 \ln J - \mu_0]\boldsymbol{f}^t + \mu_0 \boldsymbol{F}, \\ \boldsymbol{\sigma}^t &= [\lambda_t \ln J - \mu_t]\boldsymbol{I} + \mu_t \boldsymbol{b}. \end{aligned} \tag{A.2}$$

Moreover, we obtain the following explicit representations for the fourth order tangent operators $\mathbf{A}$, $\mathbf{c}$ and $\mathbf{G}$ according to Eq. (36),

$$\begin{aligned} \mathbf{A} &= \lambda_0 \boldsymbol{f}^t \otimes \boldsymbol{f}^t + \mu_0 \boldsymbol{I} \overline{\otimes} \boldsymbol{I} + [\mu_0 - \lambda_0 \ln J]\boldsymbol{f}^t \underline{\otimes} \boldsymbol{f}, \\ \mathbf{c} &= \lambda_0 \boldsymbol{I} \otimes \boldsymbol{I} + \mu_0 \boldsymbol{I} \overline{\otimes} \boldsymbol{b} + [\mu_0 - \lambda_0 \ln J]\boldsymbol{I} \underline{\otimes} \boldsymbol{I}, \\ \mathbf{G} &= \lambda_0 \boldsymbol{I} \otimes \boldsymbol{f}^t + \mu_0 \boldsymbol{F}^t \overline{\otimes} \boldsymbol{I} + [\mu_0 - \lambda_0 \ln J]\boldsymbol{I} \underline{\otimes} \boldsymbol{f}, \end{aligned} \tag{A.3}$$

whereby, in particular, $\mathbf{A} = \mathrm{D}^2_{\boldsymbol{FF}} W_0$ denotes the well-known classical tangent operator of the spatial motion problem.

A.2. Material motion problem

The internal potential energy $W_t(\boldsymbol{f})$ of the material motion problem

$$W_t = \frac{1}{2}\lambda_t \ln^2 \frac{1}{j} + \frac{1}{2}\mu_t \left[[\boldsymbol{f}^{-1} \cdot \boldsymbol{f}^{-t}] : \boldsymbol{I} - n^{\dim} - 2\ln\frac{1}{j} \right] \tag{A.4}$$

is typically parameterised in terms of the material motion deformation gradient $\boldsymbol{f}$ and its Jacobian j, with the help of the Lamé constants λ_t and μ_t. The material motion momentum fluxes $\boldsymbol{\pi}^t = \mathrm{d}_f W_t$ and $\boldsymbol{\Sigma}^t = J\boldsymbol{\pi}^t \cdot \boldsymbol{f}^t$ thus take the following format.

$$\begin{aligned} \boldsymbol{\pi}^t &= [W_t - \lambda_t \ln J + \mu_t]\boldsymbol{F}^t - \mu_t \boldsymbol{C} \cdot \boldsymbol{F}^t, \\ \boldsymbol{\Sigma}^t &= [W_0 - \lambda_0 \ln J + \mu_0]\boldsymbol{I} - \mu_0 \boldsymbol{C}. \end{aligned} \tag{A.5}$$

Finally, we can specify the fourth order tangent operators $\mathbf{a}$, $\mathbf{C}$ and $\mathbf{g}$ according to Eq. (40) as

$$\begin{aligned} \mathbf{a} &= [W_t - 2\lambda_t \ln J + 2\mu_t + \lambda_t]\boldsymbol{F}^t \otimes \boldsymbol{F}^t - [W_t - \lambda_t \ln J + \mu_t]\boldsymbol{F}^t \underline{\otimes} \boldsymbol{F} \\ &\quad - \mu_t[\boldsymbol{C} \cdot \boldsymbol{F}^t \underline{\otimes} \boldsymbol{F} + \boldsymbol{F}^t \underline{\otimes} \boldsymbol{F} \cdot \boldsymbol{C} - \boldsymbol{C} \cdot \boldsymbol{F}^t \otimes \boldsymbol{F}^t - \boldsymbol{F}^t \otimes \boldsymbol{C} \cdot \boldsymbol{F}^t + \boldsymbol{C} \overline{\otimes} \boldsymbol{b}], \\ \mathbf{C} &= [W_t - 2\lambda_t \ln J + 2\mu_t + \lambda_t]\boldsymbol{I} \otimes \boldsymbol{I} - [W_t - \lambda_t \ln J + \mu_t]\boldsymbol{I} \underline{\otimes} \boldsymbol{I} \\ &\quad - \mu_t[\boldsymbol{C} \underline{\otimes} \boldsymbol{I} + \boldsymbol{I} \underline{\otimes} \boldsymbol{C} - \boldsymbol{C} \otimes \boldsymbol{I} - \boldsymbol{I} \otimes \boldsymbol{C} + \boldsymbol{C} \overline{\otimes} \boldsymbol{I}], \\ \mathbf{g} &= [W_t - 2\lambda_t \ln J + 2\mu_t + \lambda_t]\boldsymbol{I} \otimes \boldsymbol{F}^t - [W_t - \lambda_t \ln J + \mu_t]\boldsymbol{I} \underline{\otimes} \boldsymbol{F} \\ &\quad - \mu_t[\boldsymbol{b} \underline{\otimes} \boldsymbol{F} + \boldsymbol{I} \underline{\otimes} \boldsymbol{b} \cdot \boldsymbol{F} - \boldsymbol{b} \otimes \boldsymbol{F}^t - \boldsymbol{I} \otimes \boldsymbol{F}^t \cdot \boldsymbol{b} + \boldsymbol{F} \overline{\otimes} \boldsymbol{b}] \end{aligned} \tag{A.6}$$

with $\mathbf{a} = \mathrm{d}^2_{ff} W_t$ denoting the tangent operator of the material motion problem.

Remark 11 (*Spatial vs. material quantities*). The corresponding internal potential energies W_0 and W_t, and the Lamé constants λ_0 and λ_t as well as μ_0 and μ_t

$$W_t = jW_0 \quad \lambda_t = j\lambda_0 \quad \mu_t = j\mu_0 \tag{A.7}$$

are related according to the above–stated transformation formulae.

References

[1] J. Donéa, P. Fasoli-Stella, S. Giuliani, Lagrangian and Eulerian finite element techniques for transient fluid–structure interaction problems, in: T.A. Jaeger, B.A. Boley (Eds.), Transactions of the 4th International Conference on Structural Mechanics in Reactor Technology—Volume B: Thermal and Fluid/Structure Dynamics Analysis, North-Holland Publishing Company, 1977, pp. B 1/2: 1–12.

[2] T. Belytschko, J.M. Kennedy, Computer models for subassembly simulation, Nucl. Engrg. Des. 49 (1978) 17–38.

[3] J. Donéa, Finite element analysis of transient dynamic fluid–structure interaction, in: J. Donéa (Ed.), Advanced Structural Dynamics, Applied Science Publishers, London, 1980, pp. 255–290.

[4] J. Donéa, Arbitrary Lagrangian Eulerian finite element methods, in: T. Belytschko, T.J.R. Hughes (Eds.), Computer Methods for Transient Analysis, Elsevier Science Publishers, 1983, pp. 473–516.

[5] T.J.R. Hughes, W.K. Liu, T.K. Zimmermann, Lagrangian–Eulerian finite element formulation for viscous flows, Comput. Methods Appl. Mech. Engrg. 29 (1981) 329–349.

[6] W.K. Liu, Finite element procedures for fluid–structure interactions and application to liquid storage tanks, Nucl. Engrg. Des. 65 (1981) 221–238.

[7] A. Huerta, F. Casadei, New ALE application in non-linear fast-transient solid dynamics, Engrg. Comput. 11 (1994) 317–345.

[8] T. Belytschko, W.K. Liu, B. Moran, Nonlinear Finite Element Analysis for Continua and Structures, John Wiley & Sons, 2000.

[9] W.A. Wall, Fluid-Struktur-Interaktion mit stabilisierten Finiten Elementen, Ph.D. thesis, Bericht des Instituts fur Baustatik Nr. 31, Universitat Stuttgart, 1999.

[10] H. Braess, P. Wriggers, Arbitrary Lagrangian Eulerian finite element analysis for free surface flow, Comput. Methods Appl. Mech. Engrg. 190 (2000) 95–109.
[11] A. Rodríguez-Ferran, A. Perez-Foguet, A. Huerta, Arbitrary Lagrangian–Eulerian (ALE) formulation for hyperelastoplacitcity, Int. J. Numer. Methods Engrg. 53 (2002) 1831–1851.
[12] J. Donéa, A. Huerta, Finite Element Methods for Flow Problems, John Wiley & Sons, Chichester, New York, 2003.
[13] E. Kuhl, S. Hulshoff, R. de Borst, An arbitrary Lagrangian Eulerian finite-element approach for fluid–structure interaction phenomena, Int. J. Numer. Methods Engrg. 57 (2003) 117–142.
[14] G. Pijaudier-Cabot, L. Bodé, A. Huerta, Arbitrary Lagrangian–Eulerian finite element analysis of strain localization in transient problems, Int. J. Numer. Methods Engrg. 38 (1995) 4171–4191.
[15] H. Askes, A. Rodríguez-Ferran, A. Huerta, Adaptive analysis of yield line patterns in plates with the arbitrary Lagrangian–Eulerian method, Comput. Struct. 70 (1999) 257–271.
[16] H. Askes, Advanced spatial discretisation strategies for localised failure. Mesh adaptivity and meshless methods, Ph.D. thesis, Technische Universiteit Delft, Delft, The Netherlands, 2000.
[17] H. Askes, L.J. Sluys, Remeshing strategies for adaptive ALE analysis of strain localisation, Eur. J. Mech. A: Solids 51 (2000) 447–467.
[18] H. Askes, A. Rodríguez-Ferran, A combined rh-adaptive scheme based on domain subdivision. Formulation and linear examples, Int. J. Numer. Methods Engrg. 51 (2001) 253–273.
[19] H. Askes, E. Kuhl, P. Steinmann, Arbitrary Lagrangian–Eulerian (ALE) mesh optimization by equilibration of discrete material forces, in: E. Onate, D.R.J. Owen (Eds.), Proceedings of 'COMPLAS VII', Barcelona, Spain, 07.–10. April 2003, CIMNE, Barcelona, Spain, 2003.
[20] T. Yamada, F. Kikuchi, An arbitrary Lagrangian–Eulerian finite element method for incompressible hyperelasticity, Comput. Methods Appl. Mech. Engrg. 102 (1993) 149–177.
[21] F. Armero, E. Love, An arbitrary Lagrangian–Eulerian finite element method for finite strain plasticity, Int. J. Numer. Methods Engrg. 35 (2003) 737–766.
[22] G.A. Maugin, Material Inhomogeneities in Elasticity, Chapman & Hall, London, 1993.
[23] M.E. Gurtin, Configurational Forces as Basic Concepts of Continuum Physics, Springer Verlag, New York, Berlin, Heidelberg, 2000.
[24] R. Kienzler, G. Herrmann, Mechanics in Material Space with Applications to Defect and Fracture Mechanics, Springer Verlag, Berlin, Heidelberg, New York, 2000.
[25] M. Silhavý, The Mechanics and Thermodynamics of Continuous Media, Springer Verlag, New York, Berlin, Heidelberg, 1997.
[26] G.A. Maugin, Material forces: Concepts and applications, Appl. Mech. Rev. 48 (1995) 213–245.
[27] M.E. Gurtin, On the nature of configurational forces, Arch. Rat. Mech. Anal. 131 (1995) 67–100.
[28] R.T. Shield, Inverse deformation results in finite elasticity, ZAMP 18 (1967) 490–500.
[29] P. Steinmann, Application of material forces to hyperelastostatic fracture mechanics. I. Continuum mechanical setting, Int. J. Solids Struct. 37 (2000) 7371–7391.
[30] P. Steinmann, On spatial and material settings of hyperelastodynamics, Acta Mech. 156 (2002) 193–218.
[31] P. Steinmann, On spatial and material settings of thermo-hyperelastodynamics, J. Elasticity 66 (2002) 109–157.
[32] P. Steinmann, On spatial and material settings of hyperelastostatic crystal defects, J. Mech. Phys. Solids 50 (2002) 1743–1766.
[33] E. Kuhl, P. Steinmann, On spatial and material settings of thermo-hyperelastodynamics for open systems, Acta Mech. 160 (2003) 179–217.
[34] J.D. Eshelby, The force on an elastic singularity, Philos. Trans. R. Soc. London 244 (1951) 87–112.
[35] J.D. Eshelby, The elastic energy-momentum tensor, J. Elasticity 5 (1975) 321–335.
[36] M. Braun, Configurational forces induced by finite-element discretization, Proc. Estonian Acad. Sci. Phys. Math. 46 (1997) 24–31.
[37] R. Mueller, G.A. Maugin, On material forces and finite element discretizations, Comput. Mech. 29 (2002) 52–60.
[38] P. Thoutireddy, M. Ortiz, A variational Arbitrary Lagrangian–Eulerian (VALE) method of mesh adaption and optimization in static finite-element calculations, Int. J. Numer. Methods Engrg. 53 (6) (2002) 1337–1351.
[39] P. Thoutireddy, Variational arbitrary Lagrangian–Eulerian method, Ph.D. thesis, California Institute of Technology, Passadena, California, 2003.
[40] H. Askes, E. Kuhl, P. Steinmann, An ALE formulation based on spatial and material settings of continuum mechanics. Part 2: Classification and applications, Comput. Methods Appl. Mech. Engrg., next article in this issue.